Real-Time Monitoring of Transferrin-Induced Endocytic Vesicle Formation by Mid-Infrared Surface Plasmon Resonance

Victor Yashunsky,[§] Simcha Shimron,[†] Vladislav Lirtsman,[§] Aryeh M. Weiss,[‡¶] Naomi Melamed-Book,[‡] Michael Golosovsky,[§] Dan Davidov,[§] and Benjamin Aroeti[†*]

[†]Department of Cell and Animal Biology, [‡]Confocal Unit, The Alexander Silberman Institute of Life Sciences, and [§]Racah Institute of Physics, The Hebrew University of Jerusalem, Givat Ram, Jerusalem 91904, Israel; and [¶]School of Engineering, Bar Ilan University, Ramat Gan 52900, Israel

ABSTRACT We report on the application of surface plasmon resonance (SPR), based on Fourier transform infrared spectroscopy in the mid-infrared wavelength range, for real-time and label-free sensing of transferrin-induced endocytic processes in human melanoma cells. The evanescent field of the mid-infrared surface plasmon penetrates deep into the cell, allowing highly sensitive SPR measurements of dynamic processes occurring at significant cellular depths. We monitored in real-time, infrared reflectivity spectra in the SPR regime from living cells exposed to human transferrin (Tfn). We show that although fluorescence microscopy measures primarily Tfn accumulation in recycling endosomes located deep in the cell's cytoplasm, the SPR technique measures mainly Tfn-mediated formation of early endocytic organelles located in close proximity to the plasma membrane. Our SPR and fluorescence data are very well described by a kinetic model of Tfn endocytosis, suggested previously in similar cell systems. Hence, our SPR data provide further support to the rather controversial ability of Tfn to stimulate its own endocytosis. Our analysis also yields what we believe is novel information on the role of membrane cholesterol in modulating the kinetics of endocytic vesicle biogenesis and consumption.

INTRODUCTION

All hydrophilic drugs, including protein drugs, must at some point interact with the plasma membrane as a biological barrier to be traversed en route to their target, e.g., the cell cytoplasm. A major route by which these molecules may access the cell interior is endocytosis. Therefore, a significant challenge for modern pharmacological science is to develop new technologies capable of real-time monitoring of protein trafficking into living cells. These technologies may greatly assist the development of novel strategies aiming at increasing the efficacy of protein drugs' internalization into cells, and accordingly increasing their potency as therapeutic agents to treat human diseases (see Bareford and Swaan (1) and Watson et al. (2) for reviews).

Iron is an essential nutrient that participates in numerous biological processes, primarily as a cofactor in enzymes that perform electron oxidation-reduction reactions. Transferrin (Tfn) is an important iron carrier in the body, and nearly all extracellular iron is bound to Tfn. Cellular capture of Tfn is mediated primarily by the Tfn receptor (TfnR), which is internalized via clathrin-mediated endocytosis. Recently, the Tfn endocytic pathway has been exploited for mediating delivery of therapeutic drugs, peptides, proteins, and even genes into malignant tissues and cells (3). This underscores the importance of studying the endocytic pathway of Tfn.

The TfnR has been traditionally thought to be a constitutively endocytosing receptor, i.e., a receptor whose endocytosis is not dependent on the presence of ligand. Although the empty receptor is indeed efficiently internalized via clathrin-coated pits, accumulating evidence suggests that Tfn binding may regulate certain aspects of the TfnR endocytic pathway. First, Tfn addition stimulates TfnR internalization (4); second, time-resolved capacitance measurements suggest that cell exposure to Tfn stimulates the production of endocytic vesicles (5–7); third, Tfn stabilizes the assembly, growth, and budding of clathrin-coated pits (8). Hence, the mechanism by which Tfn affects its own endocytosis definitely merits further investigation.

We reported previously that the surface plasmon resonance (SPR) in the near infrared (IR) wavelength range can be used for real-time sensing of the cell membrane cholesterol contents (9). The surface plasmon (SP) is an electromagnetic wave that propagates along a metal-dielectric interface and decays exponentially in a direction perpendicular to the interface, $E = E_0\exp(-k_z z)\cos(k_x x)$, where k_z and k_x stand for wave vectors in z and x directions (10,11). SPR applications for bioanalysis continue to grow (12,13) In the visible and near-IR range, the penetration depth, δ_z, of the SP wave is very small ($\delta_z = 0.2$–0.5 μm), thus limiting the ability of SPR to detect processes occurring close to cell-substrate contact sites. Recently, we have extended the SP technology to the mid-infrared (mid-IR) wavelength range (14), using a Fourier transform infrared spectrometer (FTIR). Because $\delta_z \sim \lambda^2$ (15), the extension to longer wavelengths enables deeper penetration of the SP field into the cell, thus allowing the sensing of dynamic processes taking place in significant portions of the cell. Because Tfn internalization via the clathrin-coated pits pathway is well

Submitted January 18, 2009, and accepted for publication May 28, 2009.

*Correspondence: aroeti@cc.huji.ac.il

Editor: Feng Gai.

© 2009 by the Biophysical Society

0006-3495/09/08/1003/10 $2.00

doi: 10.1016/j.bpj.2009.05.052

characterized, and because this pathway is significant for Tfn delivery into cells for therapeutic purposes, we decided to test the ability of the FTIR-SPR in the mid-IR to sense endocytic processes mediated by Tfn bound to its cell surface receptor. In this study, we chose the wavelength $\lambda = 2.26\ \mu$m. At this wavelength, the SP penetration depth ($\delta_z = 1.6\ \mu$m (15)) is large enough to enable detection of endocytic-related processes taking place not only at the cell's plasma membrane, but also deeper in the cytoplasm.

We found that FTIR-SPR in the mid-IR can detect, in real-time, endocytic processes related to Tfn-induced formation of early endocytic vesicles. Our SPR results correlate with independent time-resolved capacitance data (5–7), suggesting that the SP wave indeed senses Tfn-induced generation of endocytic carriers. Novel information was obtained about the cholesterol dependent dynamics of endocytic vesicle formation and consumption, e.g., by recycling back to the plasma membrane. To the best of our knowledge, our work reports for the first time that the FTIR-SPR can serve as a tool for real-time and label-free sensing of endocytic processes in living cells.

MATERIALS AND METHODS

FTIR-SPR measurements

Experimental setup

Surface plasmon was excited using Kretchmann's geometry (see Fig. S1 *A* in the Supporting Material). A Bruker FTIR spectrometer (Equinox 55, Bruker Optik GmbH, Ettlingen, Germany), equipped with a KBr beam splitter, served as the mid-IR source. A right-angle ZnS prism (20 × 40 mm base; ISP Optics, Irvington, NY) was coated with an 18-nm-thick gold film, using electron-beam evaporation. Cells were cultured on the gold surface, as described below. The prism and cells were attached to a flow chamber mounted on a goniometer, in such a way that the cells on the gold-coated surface faced the flow chamber's volume (0.5 mL). The flow chamber was filled with cell growth medium, resulting in direct contact between the medium and the cells. The growth medium was held at the temperature equal to that of the flow cell. It was passed through the chamber at a constant flow rate (5 μL/min) during the entire experiment, using a motorized bee syringe pump equipped with a variable speed controller. The infrared light from the output window of the FTIR instrument passed through a collimator, consisting of a 1-mm diameter pinhole mounted between two gold-coated off-axis parabolic mirrors with focal lengths of 76.2 mm and 25.4 mm, correspondingly. The collimated beam of 4 mm in diameter was passed through a grid polarizer and iris, reflected from the ZnS prism, and focused by an additional parabolic mirror onto a liquid-nitrogen-cooled MCT (HgCdTe) detector. We measured SPR reflectivity spectra, and monitored time dependence of the reflected beam intensity at a fixed wavelength (2.26 μm).

Cell culture preparation for SPR measurements

Human melanoma (MEL 1106) cells were cultured on a 10-cm diameter dish in Dolbecco's modified Eagle's medium (DMEM, Biological Industries, Beit Haemek, Israel), supplemented with 4.5 g/L D-glucose, 10% antibiotics, and 10% fetal calf serum, as described previously for HeLa cells (9). For SPR experiments, we cultured these cells on Au-coated prisms as follows: on reaching 70% confluence, cells were detached from the dish by trypsin C (0.05% Trypsin/EDTA in Puck's saline A; Biological Industries) treatment, and brought to a cell density of ~1.8×10^5 cells/ml in complete growth medium. Three milliliters of cell suspension were seeded on top of the Au-coated ZnS prism mounted in the home-made polycarbonate holder (Fig. S1 *B*), and as a result the cell suspension completely covered the prism's base. Cells were allowed to attach for at least 3 h in the CO_2 incubator (5% CO_2, 37°C, 90% humidity). Thereafter, growth medium (5 mL) was added, and the prism was placed in a CO_2 incubator for another 2 days until a uniform and nearly confluent cell monolayer (~30 cells per 1000 μm^2) covered the Au-surface (Fig. S1 *C*). Quantitative immunoblotting analysis, using the H68.4 anti-human TfnR monoclonal antibodies (16,17), showed similar levels of the ~90-kDa protein band corresponding to the molecular mass of the human TfnR in HeLa (cervical carcinoma cells), A431 (epidermoid carcinoma cells), and the melanoma cell-lines (Fig. S3). Because the human melanoma cells grew more consistently as a uniform and tight monolayer on the gold film, these cells were chosen as the experimental cell system for our studies.

SPR measurements and analysis

In the initial phase of each experiment, cells cultured on a gold-coated prism were exposed to serum-free DMEM for 3 h at 37°C to deplete the cells of internal pools of Tfn contributed by the serum. The prism with cells was then attached to the flow chamber, which was rapidly filled with prewarmed (37°C) minimal essential medium (MEM) containing Hank's salts (Biological Industries), 20 mM Hepes, pH 7.2, and 5 μg/mL BSA (MEM-BSA). The temperature in the flow chamber was adjusted to 37°C ± 0.1°C, unless otherwise indicated.

Thereafter, the angle of incidence in our SPR configuration was set to $\theta = 35.5°$. Measurements at this angle yielded an SPR reflectivity minimum at $\lambda = 2.34\ \mu$m ($\nu = 4280\ cm^{-1}$; Fig. 1, *inset*). Our studies were carried out close to this wavelength, i.e., at $\lambda = 2.26\ \mu$m ($\nu = 4225\ cm^{-1}$), whereby the sensitivity ($S = \Delta R/\Delta n$) is maximal. The SPR signal is the ratio of the reflectivities obtained for *p*- and *s*-polarized incident beams. The FTIR setup measured the reflectivity spectra every 25 s with a 4-cm^{-1} wavenumber resolution and with 16-scan averaging. These measurements were carried out continuously for 15–20 min, during which the MEM-BSA flow rate was 5 μL/min, until a stable SPR signal was recorded. Then, 2 mL of

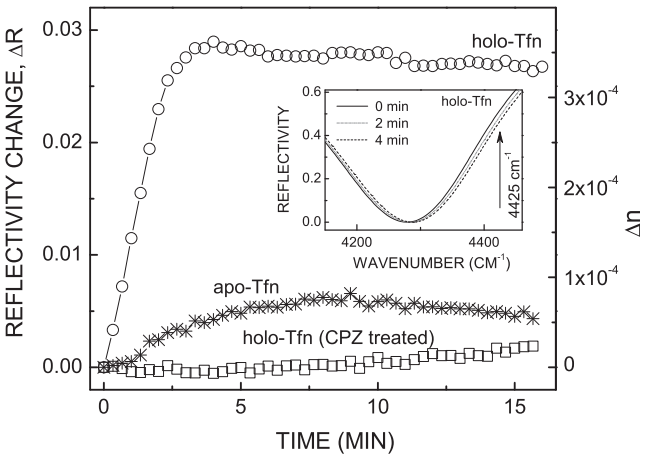

FIGURE 1 Kinetics of the SPR signal change after exposure of human melanoma cells to Tfn. Human melanoma cells cultured on a gold-coated ZnS prism were exposed to holo-Tfn (*circles*), apo-Tfn (*stars*), or first treated with CPZ followed by washout with plain MEM/BSA and then treated with holo-Tfn (*squares*). Time-resolved reflectivity in the SPR regime was recorded for each experiment independently. Left vertical scale shows reflectivity change at 4425 cm^{-1} ($\lambda = 2.26\ \mu$m). Right vertical scale shows corresponding refractive index variation. The inset shows reflectivity spectrum as measured by FTIR. Note progressive blue shift of the SPR minimum after introduction of holo-Tfn. SPR minimum is achieved at 4280 cm^{-1} and the maximal reflectivity change occurs at 4425 cm^{-1} (marked with an *arrow*).

MEM buffer containing 5 μg/mL of Tfn were introduced into the flow chamber. This step was carried out at higher flow rate (500 μL/min). In the next step, the flow rate was reduced back to 5 μL/min. SPR measurements were carried out continuously throughout all the indicated stages. At the end of each experiment, the prism was examined under the microscope for cell monolayer integrity.

Fig. S2 shows changes in the SPR reflectivity spectra recorded from a gold-coated prism, without cells (Fig. S2, *dashed line*) or with a cell layer (Fig. S2, *solid line*). The presence of cells shifts the SPR minimum to a longer wavelength, because the refractive index of cells exceeds that of the growth medium. Representative SPR signals obtained for melanoma cell monolayers exposed to holo-Tfn at 37°C and monitored at three different time points are presented in the inset of Fig. 1. The reflectivity minimum shifts toward shorter wavelengths over time due to variation of the refractive index of the medium sensed by the SPR. All subsequent results are presented as changes in reflectivity R over time $[\Delta R|_\nu = R(t_0)|_\nu - R(t)|_\nu]$, measured at a specific wavenumber $\nu = 4425\ \mathrm{cm}^{-1}$ (Fig. 1, *inset*, indicated by an *arrow*). Δn was calculated using the expression: $\Delta n = \Delta R|_\nu / S(\nu)$, where $S(\nu) = \delta R/\delta n$ is the SPR sensitivity. Specifically, $S(\nu = 4425\ \mathrm{cm}^{-1}) \approx 80\ \mathrm{RIU}^{-1}$ (refractive index units) (14).

Preparation of holo- and apo-Tfn

Human apo-Tfn (Biological Industries, Beit Haemek, Israel) was loaded with iron as described (18). The apo-Tfn was extensively dialyzed against 35 mM sodium citrate, pH 5.0, to remove possible iron traces from the commercial product. The protein was then dialyzed against 20 mM Hepes, 150 mM NaCl, pH 7.4, and used as apo-Tfn in the SPR experiments. All samples were aliquoted and frozen at −70°C.

Preparation of lissamine rhodamine apo-Tfn

Apo-Tfn was tagged with lissamine rhodamine (sulforhodamine B sulfonyl chloride), as described (19). Briefly, human Apo-Tfn (4 mg/mL dissolved in 25 mM Na_2CO_3, 75 mM $NaHCO_3$, pH 9.8), was incubated at 5°C overnight with 1 mM lissamine rhodamine sulfonyl chloride (Molecular Probes, Eugene, OR), and the labeled protein was isolated by gel filtration on Sepharose G25 (Sigma-Aldrich, St. Louis, MO) pre-equilibrated with 150 mM NaCl, 20 mM MES, pH 5.3. The sample was then dialyzed against Hepes buffer, and aliquots were stored at −20°C.

Cholesterol depletion and enrichment

Acute cholesterol depletion and enrichment of cells was achieved by treating the melanoma cells with methyl-β-cyclodextrin (mβCD, C-4555; Sigma, St. Louis, MO) or mβCD loaded with cholesterol (mβCD-chol), as described previously (9). Importantly, mβCD does not penetrate into the plasma membrane or intracellular membranes. Hence, the agent extracts cholesterol primarily from the plasma membrane and possibly from juxtaposed organelles (e.g., early endosomes) that constantly communicate with that membrane. Cholesterol levels were determined biochemically on cells cultured at ~70% confluence, using the Infinity cholesterol reagent kit (402-20; Sigma). Cholesterol levels were normalized to cellular protein levels determined by the bicinchoninic acid protein assay (Pierce Biotechnology, Rockford, IL).

Time-lapse imaging of fluorescently tagged-Tfn uptake

Melanoma cells were cultured to ~50% confluence on Glass Bottom Culture dishes (35 mm dish, 14 mm Microwell; MatTek, Ashland, MA). Cells were first exposed to growth medium lacking serum for 3 h before the experiment, and then washed three times with internalization buffer (150 mM NaCl, 20 mM Hepes, pH 7.4, 1 mM $CaCl_2$, 5 mM KCl, 1 mM $MgCl_2$, 10 mM glucose). After the last wash, internalization buffer containing 0.1 μM sulforhodamine green (SRG) (Biotium, Hayward, CA) was added to the medium. Cells were imaged with an Olympus FV-1000 confocal microscope equipped with an on-scope incubator (Life Image Services, Basel, Switzerland), which controls temperature and humidity, and provides an atmosphere of 5% CO_2. A 60×/NA = 1.35 oil immersion objective was used. Because the anionic SRG does not enter intact cells, the cells appear as dark objects against a uniform fluorescent background when imaged with the confocal microscope. First, one plane of focus was acquired, and then Rhodamine Red-holo Tfn (5 μg/mL; Jackson ImmunoResearch, West Grove, PA) was introduced into the imaging buffer. Confocal images of both the SRG (Ex: 514 nm; Em: 535–565 nm) and Rhodamine Red holo-Tfn (Ex: 543 nm; Em: 560–660 nm) were acquired from the same section every 10 or 20 s. A similar protocol was used for lissamine rhodamine apo-Tfn, except that the SRG was imaged using 488-nm excitation and a 505–525-nm emission filter. The FV1000 was equipped with the Zero Drift Controller option, to maintain the same focus plane throughout the entire period of imaging. The images were processed using ImageJ (National Institutes of Health, Bethesda, MD) as follows. First, the despeckle filter (essentially a median filter with a 3 × 3 kernel) was applied to remove point noise. The SRG image was used to determine the cell boundaries. Then, the average fluorescence intensity inside the cells ($F(t)_{\mathrm{intracellular}}$) was divided by the average fluorescence intensity in a region of interest outside the cells ($\langle F(t)\rangle_{\mathrm{extracellular}}$), i.e., fluorescence signal is $I_{\mathrm{fluo}} = F(t)_{\mathrm{intracellular}}/F(t)_{\mathrm{extracellular}}$ This procedure was adopted based on the assumption that there is insignificant depletion of labeled Tfn in the medium, so that the fluorescence in the medium should remain constant. The original time lapse sequences are provided in Movie S1, Movie S2, Movie S3, Movie S4, Movie S5, and Movie S6. The ImageJ macros that were used to process the data are available on request from the authors.

RESULTS

FTIR-SPR measurements on cells exposed to holo-Tfn detect small, but significant SPR shifts

Cells cultured on the Au-coated ZnS prism were exposed to holo-Tfn, and SPR measurements were conducted as described above. Cells exposed to the ligand at 37°C exhibited time-dependent shifts of the SPR minimum toward shorter wavelengths (''blue-shift''). The signal rapidly increased for ~2–3 min ($t_{1/2}$ = 1.6 min), and leveled-off for the remaining measurement time (Fig. 1, *circles*). Addition of Tfn to the cell-free Au-coated prism had a negligible effect on the SPR signal.

Because apo-Tfn has low binding affinity to the TfnR, this ligand should not be taken up by cells (confirmed by time-lapse microscopy, see below), we expected to observe minimal SPR shifts, if at all, on cell exposure to the ligand. Indeed, compared with holo-Tfn, the SPR signal observed in response to apo-Tfn treatment was very small (Fig. 1, *stars*). This small change might be caused by residual Fe-loaded ligand in the apo-Tfn. Taken together, these results suggest that FTIR-SPR measurements sense a dynamic event evoked in response to cell exposure to holo-Tfn. Because receptor-mediated endocytosis via clathrin-coated pits is the main portal of Tfn entry into cells, we reasoned that this process contributed to the observed changes in the SPR signal. Then, saturation of the SPR signal after 4 min of holo-Tfn uptake could represent a steady-state between two balancing membrane trafficking events: ligand-induced endocytosis and recycling back to the plasma membrane.

Chlorpromazine treatment diminishes the Tfn-induced SPR signal

The cationic amphiphilic drug chlorpromazine (CPZ) inhibits clathrin coat assembly and transferrin internalization (20). To examine the effects of CPZ on holo-Tfn uptake, cells cultured on an Au/ZnS prism were first exposed to MEM/BSA containing 10 μM CPZ at 37°C for 20 min, then CPZ was washed out with plain MEM/BSA. We waited for 30 min until a stable SPR signal was obtained, and then a typical Tfn uptake experiment was carried out. The results showed that under these conditions, the SPR signal did not respond to Tfn, and remained essentially constant during the measurement time (Fig. 1, *squares*). These results suggest that endocytic processes potentially induced by cell exposure to Tfn were inhibited by CPZ treatment.

To confirm the effects of CPZ on Tfn endocytosis by an independent method, we used fluorescence time-lapse microscopy to record in real-time the internalization of Rhodamine Red-Tfn at 37°C into live melanoma cells, as described in Materials and Methods. Briefly, cells cultured on glass coverslips were exposed to fluorescently labeled holo or apo-Tfn, or first treated with CPZ followed by 30 min of drug washout, and then exposed to the holo ligand. Representative confocal images taken from a single focal plane of Movie S1, Movie S2, and Movie S3 are shown in Fig. 2 *A upper*, *middle*, and *lower panels*, correspondingly. Quantitative analysis of the accumulation of Rhodamine Red fluorescence within a confined cell area (Fig. 2 *C*) was carried out as described in Materials and Methods, and the results are shown in Fig. 2 *B*. Apo-Tfn accumulated within the cells at significantly lower efficacy than holo-Tfn. CPZ treatment severely inhibited holo-Tfn uptake into the cells. These results correlate nicely with SPR data presented in Fig. 1, suggesting that SPR indeed sensed an endocytic process.

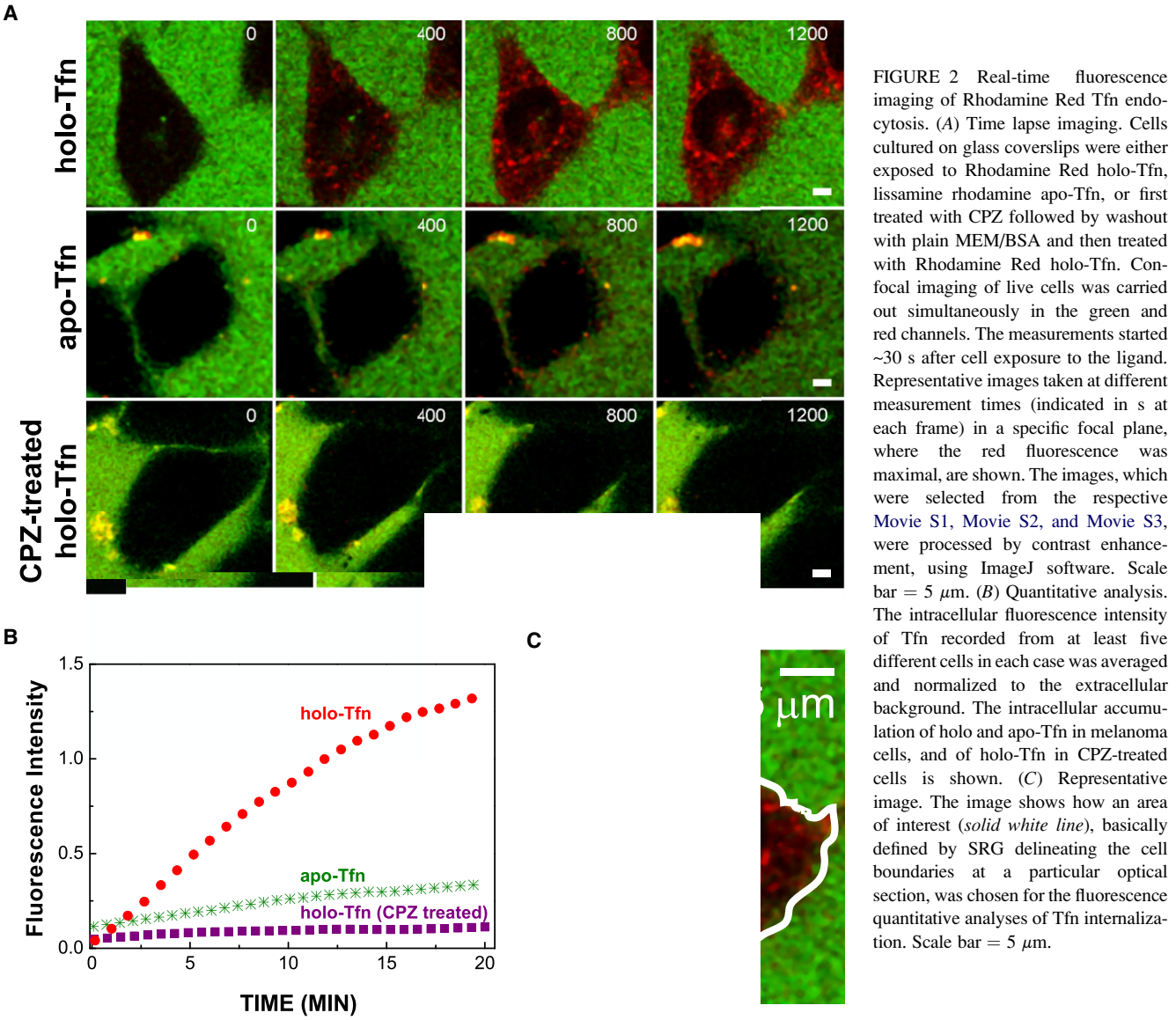

FIGURE 2 Real-time fluorescence imaging of Rhodamine Red Tfn endocytosis. (*A*) Time lapse imaging. Cells cultured on glass coverslips were either exposed to Rhodamine Red holo-Tfn, lissamine rhodamine apo-Tfn, or first treated with CPZ followed by washout with plain MEM/BSA and then treated with Rhodamine Red holo-Tfn. Confocal imaging of live cells was carried out simultaneously in the green and red channels. The measurements started ~30 s after cell exposure to the ligand. Representative images taken at different measurement times (indicated in s at each frame) in a specific focal plane, where the red fluorescence was maximal, are shown. The images, which were selected from the respective Movie S1, Movie S2, and Movie S3, were processed by contrast enhancement, using ImageJ software. Scale bar = 5 μm. (*B*) Quantitative analysis. The intracellular fluorescence intensity of Tfn recorded from at least five different cells in each case was averaged and normalized to the extracellular background. The intracellular accumulation of holo and apo-Tfn in melanoma cells, and of holo-Tfn in CPZ-treated cells is shown. (*C*) Representative image. The image shows how an area of interest (*solid white line*), basically defined by SRG delineating the cell boundaries at a particular optical section, was chosen for the fluorescence quantitative analyses of Tfn internalization. Scale bar = 5 μm.